

# Facile green biosynthesis of silver nanoparticles using *Pisum sativum* L. outer peel aqueous extract and its antidiabetic, cytotoxicity, antioxidant, and antibacterial activity

This article was published in the following Dove Press journal:  
*International Journal of Nanomedicine*

Jayanta Kumar Patra<sup>1</sup>  
Gitishree Das<sup>1</sup>  
Han-Seung Shin<sup>2</sup>

<sup>1</sup>Research Institute of Biotechnology and Medical Converged Science, Dongguk University-Seoul, Goyang 10326, Republic of Korea; <sup>2</sup>Department of Food Science & Biotechnology, Dongguk University-Seoul, Goyang 10326, Republic of Korea

**Background:** The synthesis of silver nanoparticles (AgNPs) using food waste materials and their biomedical applications have garnered considerable attention recently.

**Methods:** Here, we investigated the synthesis of AgNPs using an aqueous extract of outer peel of *Pisum sativum* under different lighting conditions using standard procedures and explored their antidiabetic, cytotoxicity, antioxidant, and antibacterial potential.

**Results:** Characterization of AgNPs was done by Ultra Violet (UV-VIS) spectroscopy that showed absorption maxima at 456 nm for the samples exposed to laboratory lighting and at 464 nm for the samples exposed to direct sunlight, by scanning electron microscopy and energy-dispersive X-ray analysis that showed the surface nature and their elemental composition with a strong peak at 3 keV that corresponded to Ag (61.85 wt%), by Fourier-transform infrared spectroscopy that predicted the functional groups involved, and by X-ray powder diffraction that showed the structural properties. The average diameter of the synthesized AgNPs was calculated to be in the range of 10–25 nm. AgNPs exhibited promising antidiabetic activity as determined by inhibition of  $\alpha$ -glucosidase (95.29% inhibition at 10  $\mu$ g/mL and IC<sub>50</sub> value of 2.10  $\mu$ g/mL) and cytotoxicity (IC<sub>50</sub> value 4.0  $\mu$ g/mL as calculated from the slope equation) against HepG2 cells. Furthermore, they also exhibited moderate antioxidant activity (50.17% reduction of 1,1-diphenyl-2-picrylhydrazyl at 100  $\mu$ g/mL) and antibacterial activity against four human pathogenic bacteria (as indicated by 8.70–11.10 mm inhibition zones on agar plates).

**Conclusion:** In conclusion, the results confirm that food waste can be used in the synthesis of AgNPs and that the latter have the potential for applications in various fields including diabetic and cancer treatments as well as in biomedicine for the manufacture of antibacterial coatings in medical devices and instruments.

**Keywords:** antibacterial, antidiabetic, antioxidant, cytotoxicity, garden pea, silver nanoparticles, *Pisum sativum*

## Introduction

Green synthesis of nanoparticles using biological materials such as extracts from various parts of the plants, algae, fungi, and a number of beneficial microorganisms is in focus in the present scientific world. The green technology method is beneficial from the conventional physical and chemical methods due to its environmentally friendly, nontoxicity, and cost-effective approach.<sup>1,2</sup> A number of

Correspondence: Han-Seung Shin  
Department of Food Science & Biotechnology, Dongguk University-Seoul, Goyangsi 10326, Republic of Korea  
Tel +82 31 961 5184  
Email spartan@dongguk.edu

studies have been reported on the synthesis of nanoparticles using the green technology approaches with the help of plant extracts, bacteria, algae, and fungi as the reducing agents in the synthesis process.<sup>1–5</sup> Silver nanoparticles (AgNPs) have recently attracted sizeable attention due to their inimitable chemical and physical properties, such as their chemical stability; thermal conductivity; photoelectrochemical activity; and high catalytic, antimicrobial, and antioxidant activities.<sup>6–8</sup> The synthesis of AgNPs using a number of biological agents including bacteria, fungi, algae, plant extracts, and byproducts has also attracted much attention.<sup>6</sup> However, the use of food waste materials and industrial wastes from the food industry in the synthesis of nanoparticles has been very limited to date.

The large amounts of byproducts produced during the processing of plant food materials amount to an economic and environmental problem due to the high volume involved and the cost of their elimination.<sup>9</sup> Aside from preventive measures to reduce the amount of waste, another –and more suitable – option is to reuse these waste materials by converting them into energy or other chemicals and materials that can be used in various applications in the food, cosmetics, and pharmaceutical industries. In light of the current situation, it would be beneficial if food waste materials could be effectively recycled and utilized as reducing agents for the synthesis of nanomaterials. Numerous attempts have been made to date to produce nanomaterials using a variety of biological and industrial waste materials as the reducing agent.<sup>10</sup> Thus, the utilization of food waste materials to synthesize various types of nanomaterials would be a highly effective, low-cost, and environmentally friendly way to recycle them for use in the generation of biomedicines and pharmaceuticals.

For pea (*Pisum sativum* L.), only the seeds are edible, while its peel is discarded as waste. The peel waste is a prime example of an undervalued and unused source of energy that can assist as the reducing agent in the synthesis of nanoparticles. It has been reported that the peel of pea is a rich source of natural bioactive compounds such as phenols and flavonoids, and it has been used in traditional medicines to treat a variety of ailments.<sup>11,12</sup> It contains a number of active compounds with antimicrobial, antioxidant, and antidiabetic potential.<sup>11,13</sup> Moreover, in countries such as India, China, Peru, and Tunisia, peas are indeed used as a treatment for diabetes.<sup>12</sup> Thus, in the present investigation, we investigated the synthesis of

AgNPs using an aqueous extract of the outer peel of garden pea and evaluated their antibacterial, antioxidant, antidiabetic, and anticancer activities.

## Materials and methods

### Preparation of sample extract

Green peas (*Pisum sativum* L.) were purchased from a local food shop in Ilsandong, Republic of Korea, and immediately taken to the laboratory for further processing. The green peas were washed thoroughly with tap water, dried with tissue paper, and the seeds were separated from the seed coat. The seed coats (the outer peel), which comprise the nonedible food component, were then cut into small pieces (Figure 1A). Approximately 25 g of the outer peels was immersed in 100 mL of deionized water in a 250-mL conical flask and boiled for 10–15 mins with continuous stirring. This was then allowed to cool to room temperature and filtered through Whatman No. 1 filter paper. The filtrate of *Pisum sativum* extract (PS extract) was collected in a clean bottle and kept at 4°C until further use.

### Biosynthesis of AgNPs using PS extract as the reducing agent

The biosynthesis of AgNPs was carried out in three different ways (under direct sunlight, under normal laboratory lighting, and in complete darkness). The experiments were carried out in triplicate and with three different sets. For each set, 100 mL aliquots of a 1 mM AgNO<sub>3</sub> aqueous solution were placed in 250-mL conical flasks, and 10 mL of the PS extract was then added dropwise with continuous stirring to each flask.<sup>14</sup> Different flasks were then exposed to different lighting conditions indicated above for the reduction process. Synthesis of the AgNPs in the solutions was visually monitored, and the changes in the color of the solutions were recorded at regular intervals followed by scanning using a UV-VIS absorption spectroscopy. The reactions were allowed to continue for 24 hrs and the solutions were then centrifuged at 10,000 rpm for 30 mins using a high-speed centrifuge. Following centrifugation, the supernatants were discarded and the pellets were washed three times with double-distilled water followed by another centrifugation step in order to remove any traces of unbound plant compounds. The pellets were collected in a crucible and dried at ambient temperature and retained for further characterization.

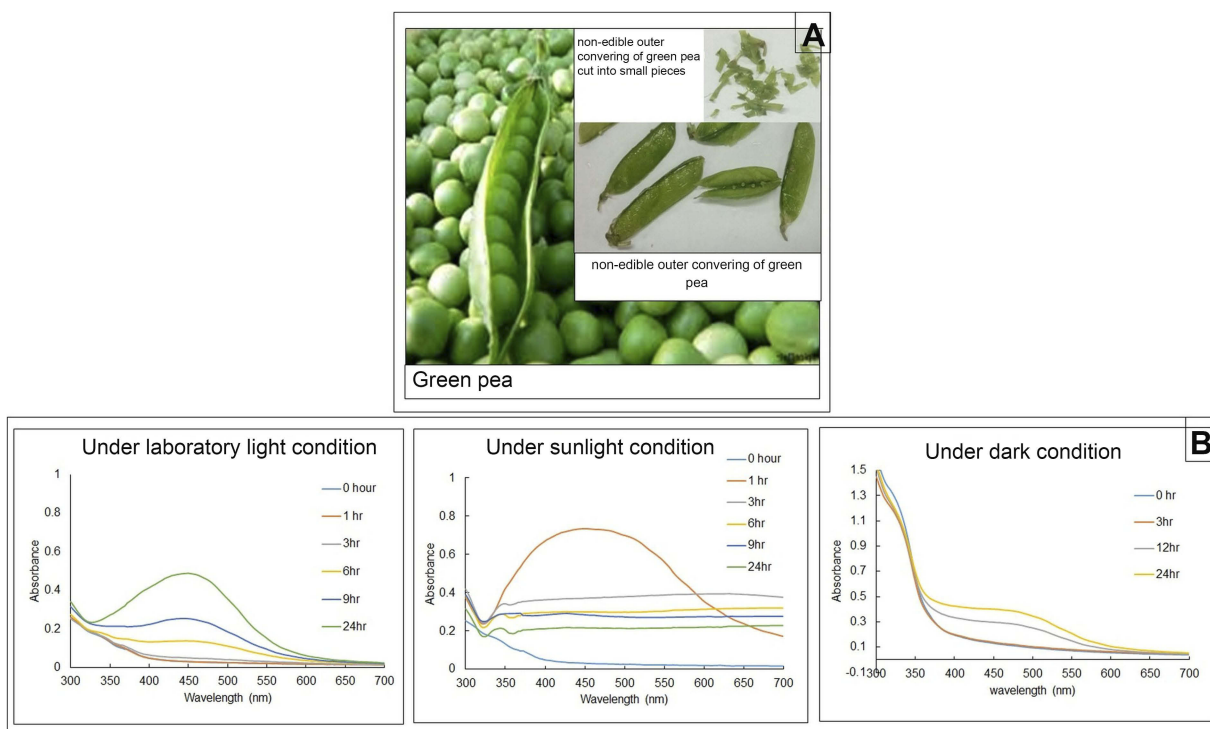


**Figure 1 (A)** Outer peel of garden pea (*Pisum sativum*) used in the synthesis of AgNPs; **(B)** Ultra Violet (UV-VIS) spectral analysis of AgNPs generated under different lighting conditions.

**Abbreviation:** AgNPs, silver nanoparticles.

## Characterization of the synthesized AgNPs

After the AgNPs had been synthesized, they were subjected to characterization of their morphological, physical, and chemical properties by various techniques including UV-VIS spectroscopy, Fourier-transform infrared spectroscopy (FT-IR), scanning electron microscopy (SEM), energy-dispersive X-ray (EDX) analysis, and X-ray powder diffraction (XRD) analysis using standard procedures.<sup>14</sup>

### UV-VIS spectroscopy

In order to study the effect of the three lighting conditions on the biosynthesis of the AgNPs, the absorption spectra of the solutions were acquired with a UV-VIS spectrophotometer (Multiskan GO; Thermo Scientific, Waltham, MA, USA) at 2-mm resolution between 300 and 700 nm for 24 hrs. Three sets of the sample taken and were analyzed for their absorption at every 1-hr time interval, at wavelengths ranging between 300 and 700 nm at each 2-nm difference. The absorption spectral values and the colors of the solutions were recorded at each time interval.

### FT-IR analysis

The FT-IR spectra of the synthesized AgNPs (generated under laboratory lighting and sunlight) and the PS extract were acquired using an FT-IR spectrophotometer (Spectrum Two™ FT-IR Spectrometer; PerkinElmer, Waltham, MA, USA) at wavelengths ranging from 400 to 4000  $\text{cm}^{-1}$ .<sup>15</sup> About 5  $\mu\text{L}$  of the sample was placed over the sample collector point of the instrument and the instrument was initiated to record the reading using the command from a specific software installed in the computer system attached to the machine. The corresponding data were recorded in the form of values in the MS Excel sheet and the respective graph was plotted.

### XRD analysis

The crystalline structure of the synthesized AgNPs was determined using an XRD device (X'Pert MRD; PANalytical, Almelo, The Netherlands) as per standard procedures.<sup>14</sup> Initially, the synthesized PS-AgNPs were powdered properly using mortar and pestle and the sample was loaded in the sample holder glass slide and fixed to the XRD machine followed by the command to run the machine using a computer interface attached to the machine. The data were

analyzed and its nature was interpreted using a specific software and computer system attached to the machine.

## SEM–EDX analysis

The surface nature and the elemental composition of the synthesized AgNPs were determined by SEM (S-4200; Hitachi, Tokyo, Japan) and EDX (EDS; EDAX Inc., Mahwah, NJ, USA) analysis. Initially, the samples were powdered properly using mortar and pestle, and a pinch of it is allowed to spread over the carbon tape attached to the sample holder. The sample holder with the sample is then sputter coated for 120 s in an ion coater machine. Then, the sample holder is placed in the SEM machine at its appropriate location in vacuum and the surface nature was analyzed by focusing the lens on the AgNPs followed by its elemental composition analysis using the EDX machine (EDS; EDAX Inc.) attached to the SEM machine. The image and data were recorded with the help of a computer system attached to the SEM machine.

## Bioactivity screening of the biosynthesized AgNPs

### Antioxidant assays

The antioxidant activity of the biosynthesized AgNPs was evaluated by the 1,1-diphenyl-2-picrylhydrazyl (DPPH) free-radical scavenging and reducing power assays. All of the assays were performed using standard procedures, and butylated hydroxytoluene (BHT) was used as the reference standard.<sup>16</sup> For the DPPH assay, the experiment was carried out in three different concentrations. Initially, 50  $\mu$ L of the sample was prepared with different concentrations of AgNPs (25–100  $\mu$ g/mL), and to it, 50  $\mu$ L of DPPH solution (0.1 mM) was added, mixed properly, and incubated in dark for 30 mins. After the incubation, the absorbance was recorded at 517 nm. BHT was taken as the reference compound. Percentage DPPH scavenging effect of the AgNPs was calculated using the following equation:

$$\text{DPPH scavenging \% age} = \frac{C - T}{C} \times 100$$

where  $C$  is the absorbance of the control value and  $T$  is the absorbance of the treatment value.

In case of the reducing assay, the reaction mixture (50  $\mu$ L) contains different concentrations of AgNPs (25–100  $\mu$ g/mL), 1%  $\text{K}_3[\text{Fe}(\text{CN})_6]$ , and 0.2 M phosphate buffer (pH 6.6). Initially, the reaction mixture was incubated at 50°C for 20 mins followed by addition of 10%  $\text{C}_2\text{HCl}_3\text{O}_2$  (50  $\mu$ L). It was then centrifuged at 1000 g, and from it, 50  $\mu$ L of the

supernatant was taken and to it 0.1%  $\text{FeCl}_3$  (10  $\mu$ L) and distilled water (50  $\mu$ L) were added and further incubated for 10 mins. The absorbance of the reaction sample was taken at 700 nm. BHT was taken as the reference standard.

### Antidiabetic assay

A standard alpha-glucosidase assay was performed to evaluate the antidiabetic potential of the synthesized AgNPs.<sup>17</sup> Initially, 20  $\mu$ g/mL of the sample was taken in the 96-well plates and serially diluted with sodium phosphate buffer (0.02 M, pH 6.9). The final volume of the solution was kept as 50  $\mu$ L followed by addition of  $\alpha$ -glucosidase (50  $\mu$ L, 0.5 U/mL). The mixture solution was mixed properly and kept for 10 mins at room temperature. Subsequently, 3 mM *p*-nitrophenylglucopyranoside (50  $\mu$ L), taken as the substrate, was added to it and further incubated for another 20 mins at 37°C. Then, 0.1 M  $\text{Na}_2\text{CO}_3$  (50  $\mu$ L) was added to the sample solution to stop the running reaction. Then, the absorbance of the reaction samples was measured at 405 nm using a plate reader. Wells with buffer, substrate, and enzyme were used as a positive control. The percentage inhibition of the enzymatic activity of  $\alpha$ -glucosidase was calculated using the following formula:

$$\text{Percentage inhibition} = \left[ \frac{C - T}{C} \right] \times 100$$

where  $C$  is the absorbance of the control sample and  $T$  is the absorbance of the “treatment” sample.

### Cytotoxicity assay

The cytotoxicity of the biosynthesized AgNPs against HepG2 cells was investigated using a standard procedure.<sup>16</sup> The cytotoxicity activity was evaluated using a commercially available EZ-Cytox kit (DoGenBio Co., Ltd., Seoul, Republic of Korea) following the manufacturer’s instructions, and the viability and the morphology of the cells were assayed by trypan blue exclusion and observation was done under an inverted microscope (DMI6000B; Leica, Wetzlar, Germany).<sup>18</sup> The HepG2 cells were purchased from Korea Cell Line Bank (Seoul, Republic of Korea). All the experiments were carried out in a 96-well plate. For the trypan blue assay, after the exposition of the cells with PS-AgNPs, the cells were thoroughly washed with the DPBS, and then 20  $\mu$ L of fresh complete DMEM and trypan blue mixture solution in 1:1 ratio were added and then the cells were visualized under the inverted microscope for the detection of live and dead cells.

## Antibacterial assay

The antibacterial activity of the biosynthesized AgNPs was tested against four different human pathogenic bacteria, namely, *Escherichia coli* O157:H7 ATCC 23514, *Enterococcus faecium* DB01, *Salmonella typhimurium* KCTC 1925, and *Salmonella enterica* KCCM 11806 using the standard disc diffusion assay.<sup>19</sup> The pathogenic bacteria were subcultured in fresh nutrient broth medium for overnight prior to use. Briefly, different concentrations of the AgNPs were prepared in 5% dimethyl sulfoxide (DMSO), and from it, the filter paper disc was prepared containing 100 µg of AgNPs/disc. Then, the pathogens were spread uniformly on the agar plates, and then the filter paper disc containing the AgNPs was placed and the plates were incubated at 37°C for overnight. Streptomycin was used as a positive control, and 5% DMSO was used as a negative control. The antibacterial activity was based on the diameter of the inhibition zone after incubation at 37°C for 24 hrs. Further, the minimum inhibitory concentration (MIC) of the AgNPs was determined by two-fold serial dilutions using standard referred procedures.<sup>20</sup> Briefly different dilutions of the AgNPs were prepared by two-fold serial dilution method, and to it, 10 µL of the pathogenic bacterial culture in nutrient broth medium was added and mixed properly, and the sample was incubated at 37°C for overnight. The minimum concentration of the sample that did not show any visible growth of the pathogenic bacteria is considered as the MIC of the AgNPs. While the value that showed complete death of the bacteria was considered as the minimum bactericidal concentration (MBC).

## Statistical analysis

The results are presented as means ± SD. One-way ANOVA was performed along with the Duncan's multiple range test using SPSS version 23.0 software (IBM Corp., Armonk, NY, USA) at a 5% level of statistical significance ( $P < 0.05$ ). Linear regression analyses and Pearson's correlation analyses were also checked to assess the association between the antioxidant parameters using the same software.

## Results

The biosynthesis of AgNPs was carried out using 1 mM AgNO<sub>3</sub> solution, with aqueous PS extract as the reducing agent and under different lighting conditions (Figure 1A). Rapid development of a change in color (to reddish brown) was observed in the samples exposed to sunlight and laboratory lighting, whereas the samples kept in

complete darkness did not exhibit any signs of reaction and there was hence no synthesis of AgNPs under the latter condition. The UV-VIS spectral analysis showed that the maximum absorbance peak was at 456 nm for the samples exposed to laboratory lighting and at 464 nm for the samples exposed to direct sunlight (Figure 1B). The only difference between these two lighting conditions was that for the samples exposed to laboratory lighting there was a steady rate of AgNP synthesis while with exposure to sunlight there was a burst of synthesis in the first hour that then tapered off over time.

The FT-IR spectral analyses of the AgNPs generated under laboratory lighting, the AgNPs generated under direct sunlight, and the PS extract are presented in Figure 2A. Absorption peaks at 3335.77, 2113.44, 1637.09, and 592.84 cm<sup>-1</sup> were observed for the PS extract, while absorption peaks at 3336.14, 2113.44, 1637.25, and 578.32 cm<sup>-1</sup> were observed for the AgNPs generated under laboratory lighting (Figure 2A). Similarly, absorption peaks at 3336.04, 2112.62, 1637.29, and 580.32 cm<sup>-1</sup> were observed for the AgNPs generated while exposed to direct sunlight (Figure 2A). The FT-IR results of the AgNPs generated under laboratory lighting and sunlight were quite similar. Thus, based on both the UV-VIS and FT-IR results, only the AgNPs generated under laboratory lighting were investigated further. The XRD spectra of the AgNPs generated under laboratory lighting are presented in Figure 4. The spectra exhibited three clear diffraction peaks at 2θ angles of 38.86, 44.29, and 64.04 that corresponded to (111), (200), and (220), respectively (Figure 2B). The surface nature and the elemental configuration of the AgNPs generated under laboratory lighting were determined by SEM-EDX analysis (Figure 2C and D). The SEM images show that the synthesized AgNPs were spherical in nature (Figure 2C, inset). By counting the average diameter of approximately 100 particles on an enlarged SEM image, the size of the particles was determined to be 10–25 nm, with an average size of 16.18 nm. Furthermore, the EDX spectra revealed the elemental composition of the AgNPs, with a strong peak at 3 keV that corresponded to Ag (61.85 wt %), thus confirming the presence of AgNPs (Figure 2D). The EDX analysis also revealed the presence of other elements such as carbon (13.83%) and oxygen (24.32%) (Figure 2D, inset).

After the characterization, the AgNPs generated under laboratory lighting were subjected to investigation of various properties including antioxidant, antidiabetic, cytotoxicity, and antibacterial activities. The antioxidant activity of the AgNPs was also investigated in terms of

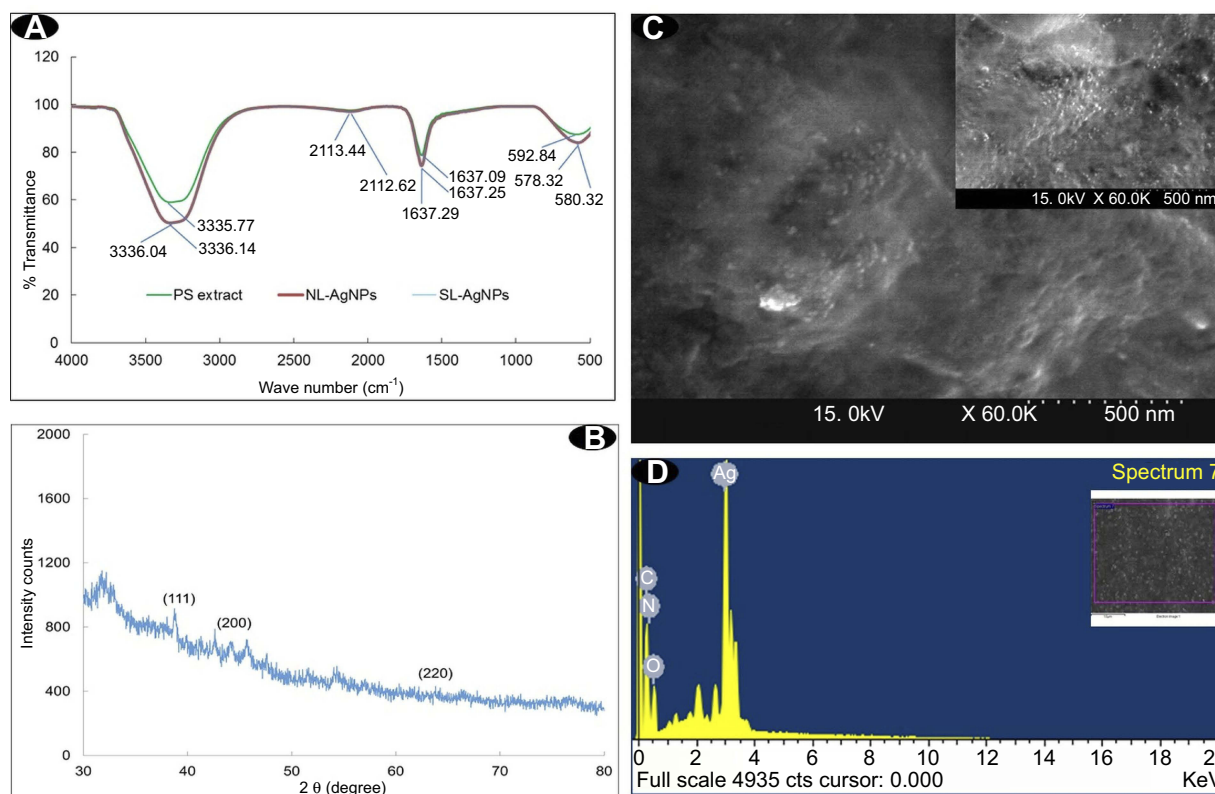


**Figure 2** (A) FT-IR spectra of the PS extract and the AgNPs synthesized under laboratory lighting (NL-AgNP) and sunlight (SL-AgNP); (B) XRD spectra; (C) SEM image; and (D) EDX spectral data.

**Abbreviations:** AgNPs, silver nanoparticles; EDX, energy-dispersive X-ray; FT-IR, Fourier-transform infrared spectroscopy; PS, *Pisum sativum*; SEM, scanning electron microscopy; XRD, X-ray powder diffraction.

their DPPH free-radical scavenging and reducing potential. The results show that the AgNPs had a moderate DPPH scavenging activity (50.17%) at 100 µg/mL compared to 90.7% scavenging activity of the BHT positive control compound (Figure 3A). However, the AgNPs exhibited a strong reducing power compared to the BHT standard reference at all three of the tested concentrations (Figure 3A). Remarkably, when the reducing power was plotted against the DPPH activity, a positive trend was observed (Figure 4), with an  $R^2$  value of 0.804 at the 95% confidence level. A stronger positive trend was also observed from the Pearson's correlation plot between the reducing power and the DPPH activity ( $r=0.897$ ) at  $P<0.01$  (Table 1). The results of the  $\alpha$ -glucosidase inhibition assay to assess the antidiabetic potential of the AgNPs are presented in Figure 3B. The results revealed an increased inhibitory activity of the AgNPs, with a maximal inhibition of 95.29% at an AgNP concentration of 10 µg/mL. Besides, the  $IC_{50}$  value of 2.10 µg/mL was found out as calculated from the slope equation ( $y=29.573x - 10.897$ ). The cytotoxicity of the AgNPs and their effect on HepG2 cell viability are presented in Figure 5.

The results show that the AgNPs had a high cytotoxicity potential, with maximum cell death with the  $IC_{50}$  value of 4.0 µg/mL as calculated from the slope equation ( $y=15.948x - 13.804$ ) (Figure 5). The morphological data obtained from the cytotoxicity assay revealed the nature of the cell death, that showed limited spreading patterns and an increased number of floating cells (black arrows) when the concentration of the AgNPs increased. Whereas the control cells and cells treated with low concentrations of AgNPs were mostly alive (white arrows) (Figure 5). The antibacterial potential of the AgNPs generated under laboratory lighting was evaluated against four different human pathogenic bacteria (*E. coli* O157:H7 ATCC 23514, *E. faecium* DB01, *S. Typhimurium* KCTC 1925, and *S. enterica* KCCM 11806) and the results are presented in Table 2. The AgNPs were active against all four of the pathogenic bacteria, with the diameter of the zones of inhibition ranging from 8.70 to 11.10 mm at concentrations of 100 µg/disc (Table 2). However, streptomycin, which acted as the positive control, resulted in inhibition zone diameters of 11.99–14.65 mm at the same concentration. The MIC of

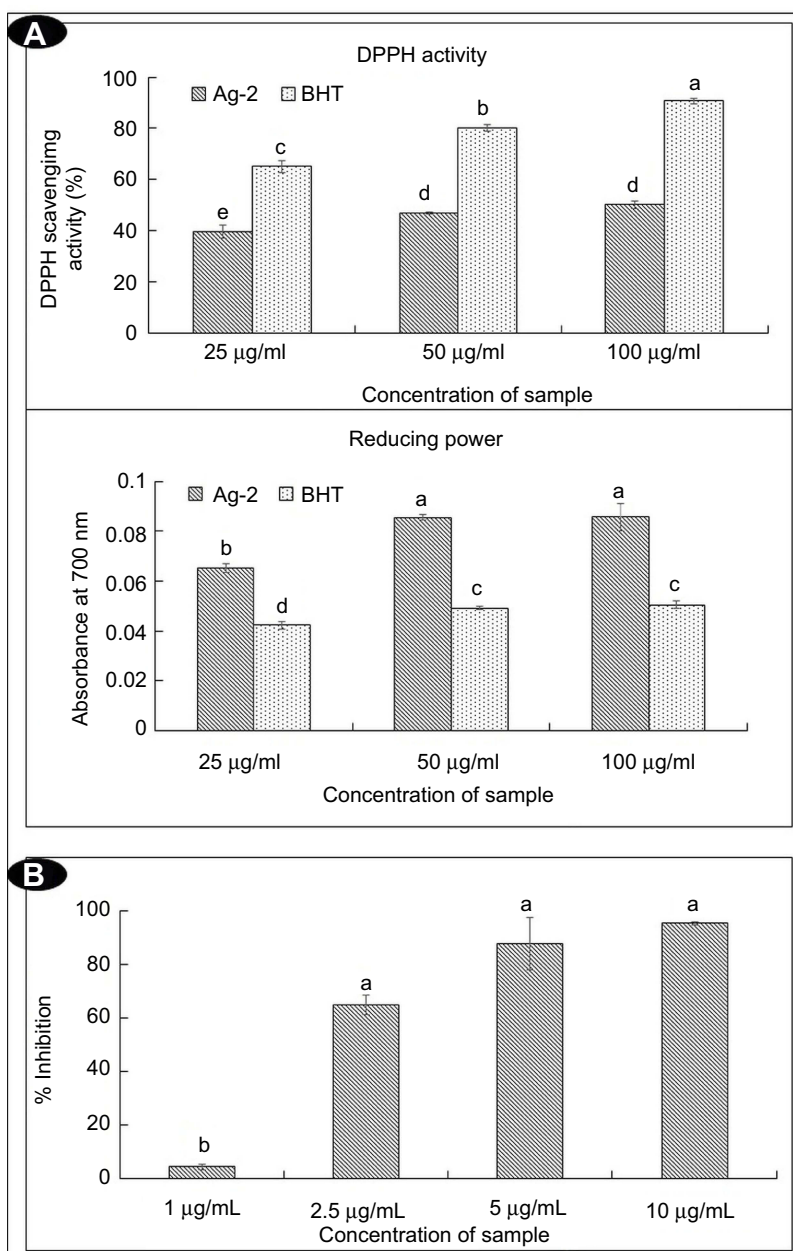


**Figure 3** (A) Antioxidant scavenging potential; (B) antidiabetic potential of the synthesized AgNPs. Difference in the superscript letters signifies statistical difference at  $P < 0.05$ . **Abbreviations:** DPPH, 1,1-diphenyl-2-picrylhydrazyl; AgNPs, silver nanoparticles.

the AgNPs against all four of the bacteria tested was determined to be  $100 \mu\text{g/mL}$ , while the MBC values were obtained as  $>100 \mu\text{g/mL}$ .

## Discussion

The synthesis of nanoparticles for various biomedical and pharmacological applications has garnered considerable attention recently, and a number of methods have been tested and developed to improve the production of environmentally suitable nanoparticles.<sup>21–23</sup> The use of plants, plant extracts,

food waste materials, and fruit peels has so far always proven to be a good substitute for reducing agents in the synthetic process as these are low-cost, safe, and nontoxic entities that are also environmentally friendly.<sup>4,16,24,25</sup> Another advantage of using biological materials in the synthetic process is that these materials are a rich source of natural bioactive compounds with numerous medicinal properties. Thus, in the current investigation, the seed coat (the outer peel) of garden peas, which is normally discarded after removal of the pea, is a food waste product that could be used as the source of the

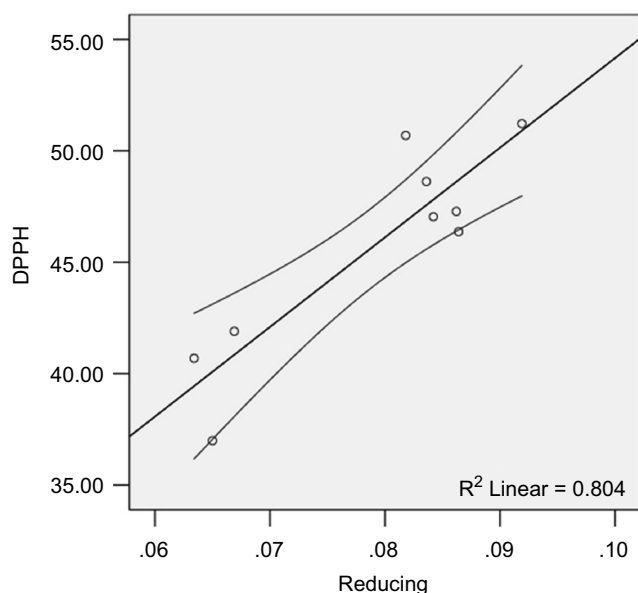


**Figure 4** Regression analysis between the DPPH and the reducing assay.  
**Abbreviation:** DPPH, 1,1-diphenyl-2-picrylhydrazyl

**Table 1** Correlation analysis between DPPH and reducing assays of AgNPs

	DPPH	Reducing
DPPH	1	0.897**
Reducing	0.897**	1

**Note:** \*\*Correlation is significant at the 0.01 level (2-tailed).

**Abbreviations:** DPPH, 1,1-diphenyl-2-picrylhydrazyl; AgNPs, silver nanoparticles.

reducing agent for the synthesis of AgNPs. It has already been reported that the outer peel of garden peas is rich in phenolic compounds and flavonoids that have important roles as the antioxidants and anticancer agents.<sup>13</sup> Moreover, there have been reports of the use of pea seed coats in folk medicines in various countries such as India, China, and Tunisia.<sup>11,12</sup>

The change in color of the reaction sample from yellowish-green to brown confirmed the completion of the AgNP synthetic process. For the three conditions that were tested, the synthetic process reached completion under both laboratory lighting and sunlight, with the former being more stable and better (Figure 1B). A possible reason for the effect of light on the synthesis of AgNPs is that the large number of photons of a particular wavelength derived from the light source may have acted as a catalyst that promoted the reduction of AgNO<sub>3</sub> to AgNPs, with the compounds in the PS extract acting as the reducing agent.<sup>26</sup> The UV-VIS absorption spectroscopy data revealed a surface plasmon resonance band due to the

excitation of free electrons at 456 nm for the samples exposed to laboratory lighting and at 464 nm for the samples exposed to sunlight (Figure 1B), which are well within the specified range reported in the literature.<sup>23,27</sup> However, in case of the sunlight-mediated synthetic process, the synthesis occurred as a burst in the first hour and then tapered off over time. This may have been due to the nonuniform exposure to photons from the sunlight, as previously reported.<sup>26</sup> The results of the FT-IR spectral analysis revealed slight shifts in the peaks of the three samples that were tested (ie, the PS extract, laboratory lighting-mediated AgNP generation, and sunlight-mediated AgNP generation). The 3335.77 cm<sup>-1</sup> band of the PS extract was shifted to 3336.14 and 3336.04 cm<sup>-1</sup> for the AgNPs generated under laboratory lighting and the AgNPs generated under direct sunlight, respectively (Figure 2A). This band is due to the O-H stretch of the H-Bond to the free hydroxyl moiety of phenol groups.<sup>28</sup> Similarly, the bands at 2113.44 and 2112.62 cm<sup>-1</sup> correspond to the -C≡C-stretch of alkynes. The band at 1637 cm<sup>-1</sup> corresponds to the N-H bend of 1<sup>ary</sup> amines, and the bands at 592.84, 580.32, and 578.32 cm<sup>-1</sup> correspond to the stretching of C-Br (alkyl halides) groups.<sup>28</sup> The slight shift in the peaks might be resulted due to the involvement of the functional groups present in the PE extract which was used as the reducing agent in the synthesis process in the reduction or stabilization of the synthesized AgNPs as discussed in previous literature.<sup>3,5</sup> The XRD spectra exhibited three clear diffraction peaks at 2θ angles of 38.86, 44.29, and 64.04 that corresponded to (111), (200), and (220), respectively (Figure 2B) and that also correspond to the face-centered cubic phase of Ag<sub>0</sub> standard (JCPDS Card no. 04-0783).<sup>29,30</sup> The SEM images revealed the spherical nature of the synthesized AgNPs, with sizes ranging from 10 to 25 nm (Figure 2C). The EDX analysis also revealed the maximum percentage of Ag, in addition to the presence of carbon and oxygen, which may be due to the use of PS extract (which is particularly rich in phenolic entities and flavonoids) as the reducing agent in the synthetic process (Figure 2D).

After completion of the synthesis and characterization of the AgNPs, they were subjected to analysis of their antioxidant, antidiabetic, cytotoxic, and antibacterial activities. The synthesized AgNPs displayed considerable reducing power and DPPH free-radical scavenging activity (Figure 3A), which can be attributed to the involvement of phenolic entities and flavonoids from the PS extract that act as reducing and capping agents in the synthetic process.<sup>31</sup> The strong positive

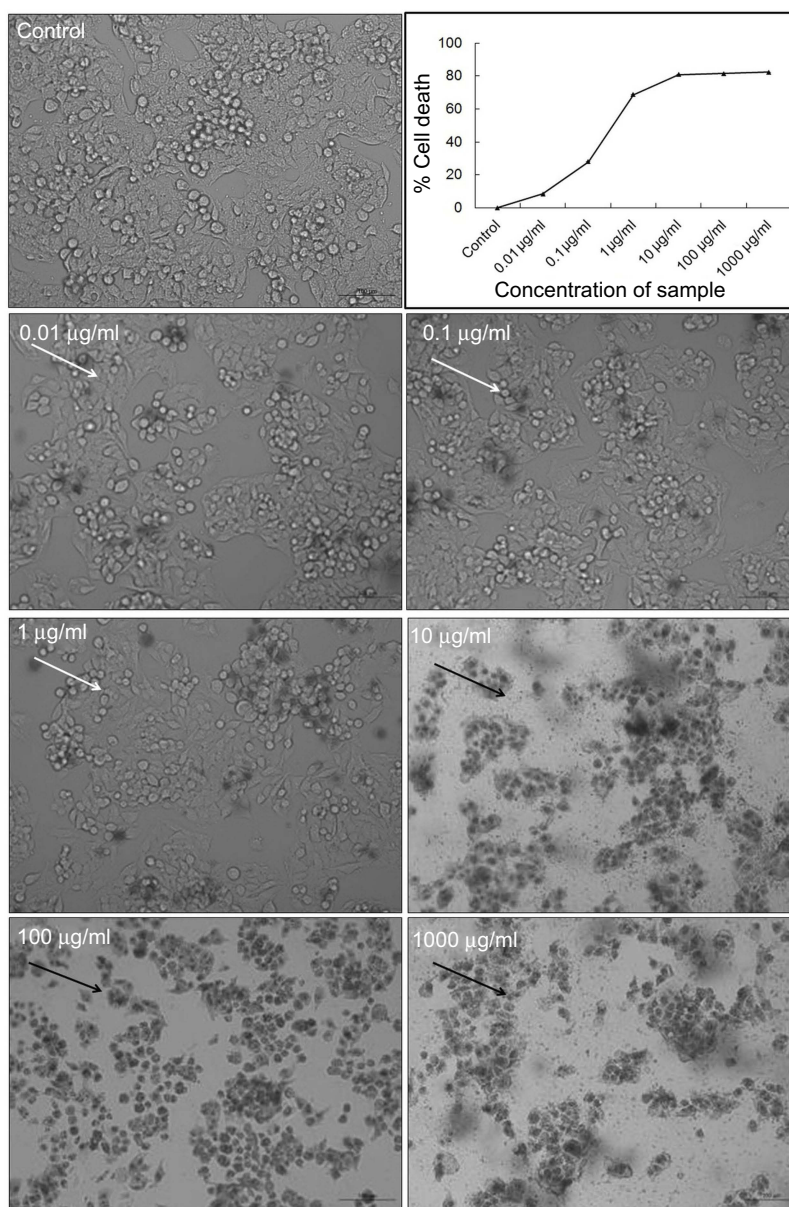


**Figure 5** Cytotoxicity activity of the synthesized AgNPs (the black arrow indicates a dead cell (floating, dark color) and the white arrow indicates a live cell (attached, faint color).  
**Abbreviation:** AgNPs, silver nanoparticles.

**Table 2** Antibacterial activity of AgNPs against four human pathogenic bacteria

Pathogen	Diameter of the zone of inhibition*	MIC (µg/mL)	MBC (µg/mL)	Streptomycin*
<i>Escherichia coli</i> O157:H7 ATCC 23514	11.10 <sup>c</sup> ±0.11	100	>100	14.65 <sup>a</sup> ±0.12
<i>Enterococcus faecium</i> DB01	9.12 <sup>d</sup> ±0.30	100	>100	12.43 <sup>b</sup> ±0.40
<i>Salmonella typhimurium</i> KCTC 1925	8.88 <sup>c,d</sup> ±0.30	100	>100	14.66 <sup>a</sup> ±0.21
<i>Salmonella enterica</i> KCCM 11806	8.70 <sup>d</sup> ±0.21	100	>100	11.99 <sup>b</sup> ±0.27

**Notes:** \*Measured in mm at a concentration of 100 µg/disc. Different superscript letters signify statistical difference at  $P < 0.05$ .

**Abbreviations:** MBC, minimum bactericidal concentration; MIC, minimum inhibitory concentration.

trend between the DPPH free-radical scavenging and the reducing activity (Figure 4, Table 1) of the AgNPs may be ascribed to the scavenging of ROS by the AgNPs, and the

positive correlation indicates that the compounds acting as capping and stabilizing agents for the AgNPs may contain phenolic functional groups. The results of these analyses

clearly indicate that the synthesized AgNPs exhibited promising antidiabetic activity in terms of their potent inhibitory activity on  $\alpha$ -glucosidase with  $IC_{50}$  value of 2.10  $\mu\text{g/mL}$  (Figure 3B). As a carbohydrate digestive enzyme of the intestine,  $\alpha$ -glucosidase plays a key role in the breakdown of polysaccharides such as oligosaccharides and disaccharides into monosaccharides, which can then readily be absorbed and cause diabetes.<sup>32,33</sup> Thus, as inhibitors of  $\alpha$ -glucosidase, it can be used to treat diabetes.<sup>33,34</sup> The synthesized AgNPs could act as a potential source for the formulation of diabetes-related drugs. Furthermore, the synthesized AgNPs also exhibited promising cytotoxicity against the HepG2 cells with an  $IC_{50}$  value of 2.0  $\mu\text{g/mL}$  (Figure 5). As suggested in previous publications, the cytotoxicity of AgNPs may be due to their very small size that may allow them to be taken up by and accumulate in cellular organelles, thereby damaging these cellular organelles and the induction of various immunological reactions.<sup>35,36</sup> It has also been suggested that the electrostatic interaction between cells and AgNPs can result in the destruction of infected cells.<sup>36,37</sup> The AgNPs described here could also serve as potential candidates for cancer treatment. Moreover, the AgNPs also exhibited moderate antibacterial activity against four human pathogenic bacteria (Table 2), which indicates that they have the potential for use in the treatment of bacterial diseases and also in biomedical applications.

## Conclusion

An aqueous extract of the outer peels of garden peas, which are normally discarded as food waste, was used as the reducing agent in the synthesis of AgNPs. Their use in nanotechnology applications could be a potential food waste utilization strategy for the management of biological wastes. Furthermore, this synthetic process is environmentally friendly, inexpensive, and largely nontoxic. The synthesized AgNPs were spherical in nature with an average size in the range of 10–25 nm. It exhibited promising antidiabetic activity as a result of their ability to potently inhibit  $\alpha$ -glucosidase with  $IC_{50}$  value of 2.10  $\mu\text{g/mL}$ , while they also exhibited high cytotoxicity activity against HepG2 cells with 4.0  $\mu\text{g/mL}$ . The AgNPs also exhibited moderate antioxidant activity in terms of DPPH free-radical scavenging and reducing power and antibacterial activity against four human pathogenic bacteria. Taken together, these results suggest that the synthesized AgNPs could serve as a promising material in the formulation of drugs to treat diabetes and cancer. Moreover, the AgNPs also have the potential for use in biomedical

applications such as in the manufacture of antibacterial coatings in medical devices and instruments.

## Acknowledgments

The authors are grateful to Dongguk University, Republic of Korea, for support. This research was supported by Korea Environmental Industry & Technology Institute (A117-00197-0703-0). The authors also wish to thank Prof. Hojun Kim and Dr. AbuZar Ansari of the Department of Rehabilitation Medicine of Korean Medicine, Dongguk University, Goyang, Republic of Korea, for cytotoxicity evaluation; Dr. C.N. Vishnuprasad, Centre for Ayurveda Biology and Holistic Nutrition, The University of Trans-Disciplinary Health Sciences and Technology (TDU), for help in antidiabetic analysis; and Dr. Anuj Kumar, School of Chemical Engineering and Department of Nano, Medical and Polymer Materials, Yeungnam University, South Korea, for help in characterization of nanoparticles.

## Disclosure

The authors report no conflicts of interest in this work.

## References

1. Patra JK, Baek K-H. Green nanobiotechnology: factors affecting synthesis and characterization techniques. *J Nanomater.* 2014;2014: Article ID 417305, 12 pages. doi:10.1155/2014/417305
2. Veerasamy R, Xin TZ, Gunasagaran S, et al. Biosynthesis of silver nanoparticles using mangosteen leaf extract and evaluation of their antimicrobial activities. *J Saudi Chem Soc.* 2011;15(2):113–120. doi:10.1016/j.jscs.2010.06.004
3. Moodley JS, Krishna SBN, Pillay K, Govender P. Green synthesis of silver nanoparticles from *Moringa oleifera* leaf extracts and its antimicrobial potential. *Adv Nat Sci.* 2018;9(1):015011.
4. Behravan M, Hossein Panahi A, Naghizadeh A, Ziaee M, Mahdavi R, Mirzapour A. Facile green synthesis of silver nanoparticles using *Berberis vulgaris* leaf and root aqueous extract and its antibacterial activity. *Int J Biol Macromol.* 2019;124:148–154. doi:10.1016/j.ijbiomac.2018.11.101
5. Pirtarighat S, Ghannadnia M, Baghshahi S. Green synthesis of silver nanoparticles using the plant extract of *Salvia spinosa* grown in vitro and their antibacterial activity assessment. *J Nanostructure Chem.* 2019;9(1):1–9. doi:10.1007/s40097-018-0291-4
6. Yu C, Tang J, Liu X, Ren X, Zhen M, Wang L. Green biosynthesis of silver nanoparticles using *Eriobotrya japonica* (Thunb.) leaf extract for reductive catalysis. *Materials.* 2019;12(1):189. doi:10.3390/ma12010189
7. Xu S, Chen S, Zhang F, et al. Preparation and controlled coating of hydroxyl-modified silver nanoparticles on silk fibers through intermolecular interaction-induced self-assembly. *Mater Des.* 2016;95:107–118. doi:10.1016/j.matdes.2016.01.104
8. Rasheed T, Bilal M, Iqbal HMN, Li C. Green biosynthesis of silver nanoparticles using leaves extract of *Artemisia vulgaris* and their potential biomedical applications. *Colloids Surf B Biointerfaces.* 2017;158:408–415. doi:10.1016/j.colsurfb.2017.07.020

9. Verma N, Bansal MC, Kumar V. Pea peel waste: a lignocellulosic waste and its utility in cellulase production by *Trichoderma reesei* under solid state cultivation. *Bioresources*. 2011;6(2):1505–1519.
10. Samaddar P, Ok YS, Kim K-H, Kwon EE, Tsang DC. Synthesis of nanomaterials from various wastes and their new age applications. *J Clean Prod*. 2018;197:1190–1209. doi:10.1016/j.jclepro.2018.06.262
11. Hadrich F, Arbi ME, Boukhris M, Sayadi S, Cherif S. Valorization of the peel of pea: *Pisum sativum* by evaluation of its antioxidant and antimicrobial activities. *J Oleo Sci*. 2014;63(11):1177–1183.
12. Gunn J, Che CT, Farnsworth N. Chapter 33 - diabetes and natural products. In: Watson RR, Preedy VR, editors. *Bioactive Food as Dietary Interventions for Diabetes*. San Diego: Academic Press; 2013:381–394.
13. El-Feky AM, Elbatanony MM, Mounier MM. Anti-cancer potential of the lipoidal and flavonoidal compounds from *Pisum sativum* and *Vicia faba* peels. *Egypt J Basic Appl Sci*. 2018;5(4):258–264. doi:10.1016/j.ejbas.2018.11.001
14. Patra JK, Baek K-H. Novel green synthesis of gold nanoparticles using *Citrullus lanatus* rind and investigation of proteasome inhibitory activity, antibacterial, and antioxidant potential. *Int J Nanomedicine*. 2015;10:7253.
15. Basavegowda N, Mishra K, Thombal RS, Kaliraj K, Lee YR. Sonochemical green synthesis of yttrium oxide (Y<sub>2</sub>O<sub>3</sub>) nanoparticles as a novel heterogeneous catalyst for the construction of biologically interesting 1, 3-thiazolidin-4-ones. *Catal Letters*. 2017;147(10):2630–2639. doi:10.1007/s10562-017-2168-4
16. Patra JK, Das G, Kumar A, Ansari A, Kim H, Shin H-S. Photo-mediated biosynthesis of silver nanoparticles using the nonedible accrescent fruiting calyx of *Physalis peruviana* L. fruits and investigation of its radical scavenging potential and cytotoxicity activities. *J Photochem Photobiol B*. 2018;188:116–125. doi:10.1016/j.jphotobiol.2018.08.004
17. Butala MA, Kukkupuni SK, Venkatasubramanian P, Vishnuprasad CN. An ayurvedic anti-diabetic formulation made from *Curcuma longa* L. and *Embllica officinalis* L. inhibits  $\alpha$ -amylase,  $\alpha$ -glucosidase, and starch digestion, in vitro. *Starch-Stärke*. 2018;70(5–6):1700182. doi:10.1002/star.201700182
18. Faedmaleki F, Shirazi FH, Salarian -A-A, Ashtiani HA, Rastegar H. Toxicity effect of silver nanoparticles on mice liver primary cell culture and HepG2 cell line. *Iran J Pharm Res*. 2014;13(1):235.
19. Diao W-R, Hu Q-P, Feng -S-S, Li W-Q, Xu J-G. Chemical composition and antibacterial activity of the essential oil from green huajiao (*Zanthoxylum schinifolium*) against selected foodborne pathogens. *J Agric Food Chem*. 2013;61(25):6044–6049. doi:10.1021/jf4007856
20. Kubo I, Fujita K-I, Kubo A, Nihei K-I, Ogura T. Antibacterial activity of coriander volatile compounds against *Salmonella choleraesuis*. *J Agric Food Chem*. 2004;52(11):3329–3332. doi:10.1021/jf0354186
21. He Y, Wei F, Ma Z, et al. Green synthesis of silver nanoparticles using seed extract of *Alpinia katsumadai*, and their antioxidant, cytotoxicity, and antibacterial activities. *RSC Adv*. 2017;7(63):39842–39851. doi:10.1039/C7RA05286C
22. He Y, Li X, Zheng Y, et al. A green approach for synthesizing silver nanoparticles, and their antibacterial and cytotoxic activities. *New J Chem*. 2018;42(4):2882–2888. doi:10.1039/C7NJ04224H
23. Mousavi B, Tafvizi F, Zaker Bostanabad S. Green synthesis of silver nanoparticles using *Artemisia turcomanica* leaf extract and the study of anti-cancer effect and apoptosis induction on gastric cancer cell line (AGS). *Artif Cells Nanomed Biotechnol*. 2018;46(sup 1):499–510.
24. Jegadeeswaran P, Shivaraj R, Venkatesh R. Green synthesis of silver nanoparticles from extract of *Padina tetrastratica* leaf. *Dig J Nanomater Biostruct*. 2012;7(3):991–998.
25. Patra JK, Baek K-H. Antibacterial activity and synergistic antibacterial potential of biosynthesized silver nanoparticles against foodborne pathogenic bacteria along with its anticandidal and antioxidant effects. *Front Microbiol*. 2017;8:167. doi:10.3389/fmicb.2017.00167
26. Srikar SK, Giri DD, Pal DB, Mishra PK, Upadhyay SN. Light induced green synthesis of silver nanoparticles using aqueous extract of *Prunus amygdalus*. *Green Sustainable Chem*. 2016;6(01):26. doi:10.4236/gsc.2016.61003
27. Sastry M, Mayya K, Bandyopadhyay K. pH Dependent changes in the optical properties of carboxylic acid derivatized silver colloidal particles. *Colloids Surf A Physicochem Eng Asp*. 1997;127(1–3):221–228. doi:10.1016/S0927-7757(97)00087-3
28. Coates J. Interpretation of infrared spectra, a practical approach. In: *Encyclopedia of Analytical Chemistry*, RA. Meyers (Ed.). John Wiley & Sons Ltd, Chichester; 2000:10881–10882.
29. Jagtap UB, Bapat VA. Green synthesis of silver nanoparticles using *Artocarpus heterophyllus* Lam. seed extract and its antibacterial activity. *Ind Crops Prod*. 2013;46:132–137. doi:10.1016/j.indcrop.2013.01.019
30. Morris MC, McMurdie HF, Evans EH, Paretzkin B, Parker HS, Panagiotopoulos NC, Hubbard CR. Standard X-ray diffraction powder patterns, National Bureau of Standards monograph 25 section 18 (Library of congress catalog card number: 53-61386). In: *National Bureau of Standards*. Washington, DC, USA: U.S. Department of Commerce, Malcolm Baldrige, Secretary, National Bureau of Standards, Ernest Ambler, Director; 1981:2.
31. Adedapo AA, Jimoh FO, Afolayan AJ, Masika PJ. Antioxidant activities and phenolic contents of the methanol extracts of the stems of *Acokanthera oppositifolia* and *Adenia gummifera*. *BMC Complement Altern Med*. 2008;8(1):54. doi:10.1186/1472-6882-8-62
32. Sales PM, Souza PM, Simeoni LA, Magalhães PO, Silveira D.  $\alpha$ -Amylase inhibitors: a review of raw material and isolated compounds from plant source. *J Pharm Pharm Sci*. 2012;15(1):141–183. doi:10.18433/J35S3K
33. Balan K, Qing W, Wang Y, et al. Antidiabetic activity of silver nanoparticles from green synthesis using *Lonicera japonica* leaf extract. *RSC Adv*. 2016;6(46):40162–40168. doi:10.1039/C5RA24391B
34. Yousefi A, Yousefi R, Panahi F, et al. Novel curcumin-based pyrano [2,3-d]pyrimidine anti-oxidant inhibitors for  $\alpha$ -amylase and  $\alpha$ -glucosidase: implications for their pleiotropic effects against diabetes complications. *Int J Biol Macromol*. 2015;78:46–55. doi:10.1016/j.ijbiomac.2015.03.060
35. Faedmaleki F, Shirazi FH, Salarian AA, Ashtiani HA, Rastegar H. Toxicity effect of silver nanoparticles on mice liver primary cell culture and HepG2 cell line. *Iran J Pharm Res*. 2014;13(1):235–242.
36. Rajkumar T, Sapi A, Das G, Debnath T, Ansari A, Patra JK. Biosynthesis of silver nanoparticle using extract of *Zea mays* (corn flour) and investigation of its cytotoxicity effect and radical scavenging potential. *J Photochem Photobiol B*. 2019;193:1–7. doi:10.1016/j.jphotobiol.2019.01.008
37. Patil Shriniwas P, T KS. Antioxidant, antibacterial and cytotoxic potential of silver nanoparticles synthesized using terpenes rich extract of *Lantana camara* L. leaves. *Biochem Biophys Rep*. 2017;10:76–81. doi:10.1016/j.bbrep.2017.03.002

## International Journal of Nanomedicine

Dovepress

### Publish your work in this journal

The International Journal of Nanomedicine is an international, peer-reviewed journal focusing on the application of nanotechnology in diagnostics, therapeutics, and drug delivery systems throughout the biomedical field. This journal is indexed on PubMed Central, MedLine, CAS, SciSearch<sup>®</sup>, Current Contents<sup>®</sup>/Clinical Medicine,

Journal Citation Reports/Science Edition, EMBase, Scopus and the Elsevier Bibliographic databases. The manuscript management system is completely online and includes a very quick and fair peer-review system, which is all easy to use. Visit <http://www.dovepress.com/testimonials.php> to read real quotes from published authors.

Submit your manuscript here: <https://www.dovepress.com/international-journal-of-nanomedicine-journal>